analytical chemistry

Article

pubs.acs.org/ac

Plasma-Enhanced Antibody Immobilization for the Development of a Capillary-Based Carcinoembryonic Antigen Immunosensor Using Laser-Induced Fluorescence Spectroscopy

Qiaoling Yu,[†,‡] Xuefang Zhan,[†] Kunping Liu,[†,§] Hao Lv,[†] and Yixiang Duan*[,†]

[†]Research Center of Analytical Instrumentation, Analytical & Testing Centre, College of Chemistry, Sichuan University, Chengdu 610064, P. R. China

[‡]Department of Environmental and Food Engineering, Liuzhou Vocational and Technical College, Liuzhou 545006, P. R. China

[§]Faculty of Biotechnology Industry, Chengdu University, Chengdu 610106, P. R. China

Supporting Information

ABSTRACT: In this study, antibody immobilization using a microwave-induced H_2O/Ar plasma pretreatment was achieved for the first time. Plasma was used to activate the surface of a capillary-based immunosensor by increasing the density of silicon hydroxyls and dangling bonds to ensure better silanization. The capture antibodies were covalently immobilized after the silanized surface reacted with glutaraldehyde and antibodies. A Cy3-labeled detection antibody was used in combination with the antigen captured by the immunosensor to complete the sandwich-type immunoassay, and the signals were measured using a laser-induced fluorescence system. Microwave-induced H_2O/Ar plasma pretreatment of the carcinoembryonic antigen (CEA) immunosensor improved the antibody immobilization, and there was an obvious improvement in the linear detection range, i.e., 1 order of magnitude compared with a commercial enzyme-linked immunosorbent assay (ELISA). This novel immobilization method dramatically improved the detection limit (0.5 pmol/L CEA) and sensitivity. Assay validation studies indicated that the correlation coefficient reached 0.9978, and the relative standard deviations were <7% for all samples, with recoveries of 99.7−107.1%. Furthermore, the immunosensor was applied successfully to CEA determination in actual saliva specimens with high sensitivity, acceptable precision, and reasonable accuracy. This enhanced CEA immunosensor based on microwave-induced H_2O/Ar plasma was demonstrated to be a sensitive tool for CEA diagnostics.

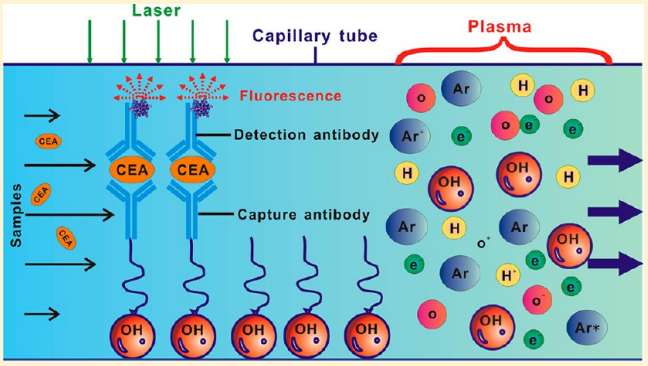

Immunosensors are powerful detection devices for quantifying small amounts of tumor markers[1] in complex diagnostic fluids, because complex separation and extraction steps are avoided and their specificity, analytical time, and practicability are ideal. Antibodies are used as highly specific recognition molecules to react with the epitopes of antigens, and a detectable response is produced for interpretation, such as fluorescence or electricity. The immobilization of the antibody on the substrate is a crucial procedure during the construction of immunosensors, which is usually achieved in three ways, i.e., physical adsorption,[2−4] covalent immobilization,[1,5−7] and bioaffinity immobilization.[8−10]

Covalent binding is the most widely applied method because of its irreversible binding and reasonable cost compared with bioaffinity immobilization. A typical antibody contains 50−70 lysine residues and several cysteine residues with functional groups, such as amine or thiol, which can be utilized as anchoring points. At the same time, the surfaces of inorganic substrates that lack sufficient active groups, including fused silica, need to be activated so antibodies cannot be attached directly. Silicon hydroxyls are potential active groups on the surface of fused silica, which can actively participate in certain chemical reactions. The maximum density reaches five silicon hydroxyls per 100 square angstroms,[11] although this cannot be achieved in normal conditions. The lack of anchoring points means that the quantity of immobilized antibodies is not sufficient, which restricts the detection sensitivity of immunosensors. Therefore, the surface of fused silica needs to be activated further using efficient methods.

Plasma treatment is an efficient technique in the field of surface modifications,[12] and our group has worked on plasma technologies for a long time.[13−17] Plasma is an ionized gas that contains charged and neutral particles,[18] such as excited species, radicals, electrons, ions, and UV light, which can interact strongly with the surfaces of substrates, thereby producing chemical and physical modifications on surfaces. Surface

Received: January 21, 2013
Accepted: April 2, 2013
Published: April 2, 2013

   dx.doi.org/10.1021/ac400226n | *Anal. Chem.* 2013, 85, 4578−4585

exposure to plasma causes an etching effect,[19,20] which induces defects,[21] charged surface states,[22,23] dangling bonds, and increased surface roughness.[22,24,25] There is a concomitant decrease in the contact angle of surfaces after treatment with oxygen-containing plasmas[19] or microwave-induced argon plasma,[24,26] which suggests that the hydrophilicity of the surface might also be enhanced. Thus, the biocompatibility of the surface may be improved for tissue engineering application[24,26] or bioactive compound immobilization.[27,28] In addition, plasma exposure can introduce a wide range of different functional groups onto the surface, depending on the plasma parameters such as the power, gases used, treatment time, and pressure.[28,29] For example, oxygen-containing groups, such as C−O, C═O, and O−C═O, were generated on the surfaces of carbon nanotubes in a microwave-excited surface-wave Ar/O_2 plasma system with a high electron density and a low electron temperature;[30] amino groups were introduced onto a fluoropolymer surface using a radiofrequency glow discharge ammonia plasma;[29] carboxylic acid, alcohols, and other oxygen-containing functionalities were introduced by plasma treatments involving CO_2, H_2O, and CO_2/H_2O or H_2/H_2O, O_2/H_2O, and H_2/O_2;[29] and hydroxyl functional groups were introduced by Ar plasma pretreatment on poly(ethylene glycol) films.[28] These experiments showed that the high density immobilization of bioactive compounds, such as L-cysteine,[28] DNA molecules,[31] and horseradish peroxidase,[27] can be achieved using plasma surface modification methods. Recent studies reported[28,32] that addition of water vapor to the plasma gases would increase the concentration of OH radicals in the plasma jet. The dominant OH formation path is Penning ionization of water molecules through dissociative recombination in the He discharge with the addition of water vapor.[32] OH radicals in the plasma grafted to dangling bonds of silica surface through collision. The surface density of OH group, i.e. anchoring points of antibody, is enhanced. Therefore, plasma modification could be used for the covalent immobilization of antibodies to produce immunosensors with a high surface coverage. To the best of our knowledge, antibody immobilization with plasma pretreatment has not been reported previously.

Carcinoembryonic antigen (CEA), a polysaccharide-protein complex, is used widely as a clinical tumor marker, and it has been evaluated in a wide range of malignancies, such as colorectal cancer, pancreatic cancer, gastric cancer, and breast cancer, and its levels may reflect the disease progression or regression status. It may also be useful during the early diagnosis of recurrences and monitoring responses to treatment. In this study, a CEA immunosensor was constructed with microwave-induced H_2O/Ar plasma pretreatment, which was used to treat fused silica capillary tubes to increase the density of silicon hydroxyls on their surfaces. These groups were then reacted with 3-(aminopropyl) triethoxysilane (APTES) to leave amine groups for conjugation with the aldehydes of the homobifunctional cross-linker, glutaraldehyde (GA). The CEA antibodies were immobilized by covalent bonds between the amine groups of lysine residues and the other aldehydes of GA. A CEA immunosensor was constructed for sandwich type immunoreactions, and signals were measured using a laser-induced fluorescence system. The detection sensitivity, linear range, and limit of detection (LOD) were all improved after the microwave-induced H_2O/Ar plasma pretreatment. Thus, this method may be used to develop sensitive and specific cancer diagnostic tools.

EXPERIMENTAL SECTION

Materials. Phosphate-buffered saline (PBS) (pH 7.4, 0.01 M) was used as a wash buffer and diluent for the protein standards, and it was sterilized and prepared fresh daily. Carbonate buffer (0.05 M, pH 9.6) was used for antibody immobilization. To maintain the protein stability and reduce nonspecific binding, bovine serum albumin (BSA; Sagon Biotec, Shanghai, China) was added at 10 mg/mL to the PBS. The detection and capture monoclonal antibody pairs, Cy3-labeled mouse antihuman CEA antibody and mouse antihuman CEA antibody, were purchased from Bioss (Beijing, China). CEA human antigen (calibrator grade) and alpha fetoprotein (AFP) were purchased from Keyuezhongkai (Beijing, China). These proteins were used without further purification and were diluted in PBS or PBS/BSA to produce the appropriate concentrations. Silica capillary tubes (1.2 mm i.d., 2 mm o.d, and 70 mm long) were purchased from Lehua Quartz (China). Human fibrinogen, L-tryptophan, L-phenylalanine, and L-valine used in interference test were purchased from Sagon Biotec (Shanghai, China). Hemoglobin and ciprofloxacin were from Blodee Biotec (Beijing, China) and Yuanye Biotec (Shanghai, China), respectively. All other reagents, including GA, APTES, and gelatin, were obtained from Kermel (Tianjin, China) and used without further purification.

Immunosensor Setup. The immunosensor setup used in this study is shown in Figure 1. A diode pumped solid-state

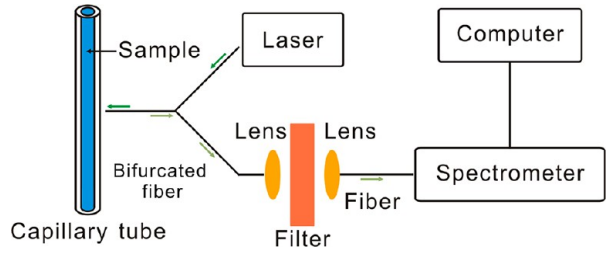

Figure 1. Schematic diagram of the laser-induced fluorescence setup.

laser (Dedo Instruments, Beijing, China) was used as the excitation light source. The excitation light (532 nm) was coupled to one leg of the bifurcated UV−vis fiber (NA = 0.22; Ocean Optics, FL, USA) and transported to the capillary via the common end of the fiber. The fluorescent photons emitted from a sample in the capillary were directly collected in the same end and filtered using a 550 nm long-pass filter from the other leg of the fiber. The fluorescence signals were measured using a high resolution spectrometer ($HR2000^+$, split = 50 μM; Ocean Optics, FL, USA) with an integration time of 200 ms and an average of three traces to ensure noise suppression.

Microwave Plasma Device. A copper Surfatron microwave cavity was used in this study, which was based on our previous work[14] with some simplified modifications. In this version of the Surfatron design, the distances between the microwave antenna, the capillary, and the major and minor tuning screws were fixed after appropriate adjustment to achieve a stable microwave discharge and to minimize the reflected power. The microwave antenna is used to couple microwave energy in the silica capillary. A quartz tube (2.0 mm i.d., 6 mm o.d, and 180 mm long) was used as a cushion layer where the capillary was centered axially. Each capillary was concentrically centered in the cylindrical Surfatron cavity, as

dx.doi.org/10.1021/ac400226n | Anal. Chem. 2013, 85, 4578−4585

shown in Figure 2. The plasma cavity was connected to a solid-state microwave generator (2.45 GHz; Yanyou Electronics, Nanjing, China) via a coaxial cable. The flow gas was introduced into the capillary where the plasma was sustained. The plasma emission signals were measured using a high resolution spectrometer (HR2000$^+$, split = 5 μM; Ocean Optics, FL, USA) with an integration time of 100 ms.

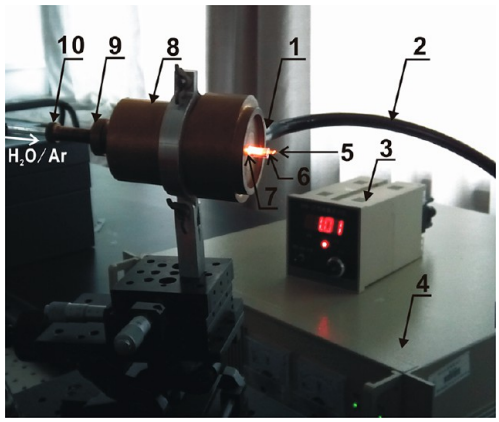

Figure 2. The microwave-induced plasma setup used for capillary pretreatment: (1) microwave antenna; (2) coaxial cable; (3) gas flow meter; (4) solid-state microwave generator; (5) plasma; (6) capillary; (7) quartz tube; (8) Surfatron plasma cavity; (9) major tuning screw; and (10) minor tuning screw.

AFM Measurements. The surface topography and roughness of the modifications of the silica slices were analyzed using an atomic force microscope (SPM/AFM 5500; Agilent, USA) in the contact mode. An n-silicon tip with a length of 225 μm scanned the surfaces at a rate of 1.0 lines/s and the two-dimensional topography images and roughness values were obtained simultaneously. The roughness values were calculated using the instrument's SPIP V software.

Assay Protocol. Capillary tubes were cleaned and hydrophilized using a 1:1 mixture of hydrochloric acid and methanol for 1 h at room temperature, washed with water, and dried in a vacuum oven. The dried capillary tubes were used immediately or stored in a vacuum desiccator.

Cleaned capillary tubes were activated by microwave induced plasma for 15 min with 1.45 L/min Ar and water vapor (2% v/v), and the voltage of the microwave power source was 5.6 V (64.3 W). The inner surfaces of capillary tubes were coated with primary amines by immediately immersing them into an 8% (v/v) APTES solution in absolute ethanol for 12 h. Next, they were washed and dried at 120 °C for 2 h. The amine groups were reacted with the homobifunctional cross-linker GA by incubating the capillary tubes in 2.5% GA water solution for 4 h and washing until there was no odor of GA. GA can bind to the amine groups on one side of an aldehyde group and form an aldehyde-activated surface on the other side. To expose the amine groups of the capture antibody, mouse antihuman CEA antibodies were diluted to 10 μg/mL using PBS. The antibody immobilization procedures were completed after the capture antibodies in carbonate buffer were injected into the capillary for coupling at 4 °C, overnight. It was expected that the capture antibody would be immobilized on the capillary tubes surfaces via covalent bonds between the other aldehyde groups of GA and the amine groups of the antibody. The capillary tubes were blocked by incubation with BSA in PBS for 6 h at 4 °C and rinsed with PBS. The capillary tubes were dried and stored in a refrigerator.

The capture antibody-modified capillary tubes were incubated for 60 min at 37 °C with a series of samples that contained either purified CEA antigen or clinical samples at various concentrations. After a thorough wash with PBS/BSA, the detection antibodies that were prepared by diluting the stock solution of Cy3-labeled mouse antihuman CEA antibody with PBS/BSA to produce a volume ratio of 1:25 were added to react with the captured CEA for 60 min at 37 °C. The unbound Cy3-labeled antibody was washed away with PBS/BSA. The fluorescent signals of the CEA immunocomplex were measured using laser-induced fluorescence spectroscopy.

Saliva Sample Collection and Pretreatment. Whole saliva samples were collected from five apparently healthy volunteers after rinsing their mouths with water, according to a standard method.[33] The saliva samples were centrifuged at 2000 r/min for 30 min, and the supernatants were collected and stored at −20 °C until analysis.

RESULTS AND DISCUSSION

Plasma Characterization and Surface Treatment. Microwave-induced H_2O/Ar plasma was used for antibody immobilization in this study. Figure 3 shows typical OES spectra for the Ar/H_2O plasma (top) with a H_2O volume/volume ratio of 2% and pure Ar plasma (bottom). The spectrum was obtained in the same plasma operating conditions as described above. The Ar emission lines show similar behaviors, which are attributed to Ar radicals, atoms, and ions. The characteristic emissions of water vapor appeared when water vapor was introduced into the Ar plasma. The excited atoms of hydrogen, oxygen, and OH radicals were identified, as shown in Figure 3. The OH emission lines around 309.3 and 314 nm are attributed to the transition OH ($A^2\Sigma^+ \rightarrow X^2\Pi_{3/2}$).[32,34,35] The H_β line (H ($n = 4 \rightarrow n = 2$)) transition is at 486.1 nm (Figure 3). It must be mentioned that the H_α emission line (656.3 nm) closely follows the trend of the H_β emission line. The oxygen atom and radical emission lines were located at 670.8, 844.6, 777.2, and 926.1 nm. In addition to the excited gas Ar and water vapor, the plasma stream may also have contained components from the environment. Thus, the

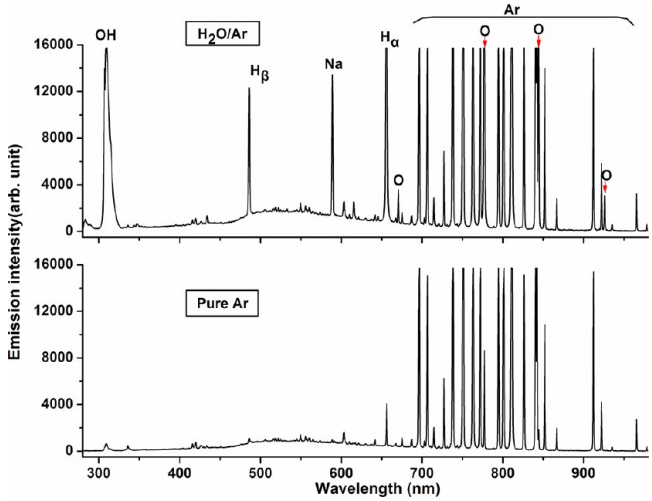

Figure 3. Typical optical emission spectra for Ar plasma (bottom) and H_2O/Ar plasma (top) with H_2O volume/volume ratios of 2%.

dx.doi.org/10.1021/ac400226n | Anal. Chem. 2013, 85, 4578−4585

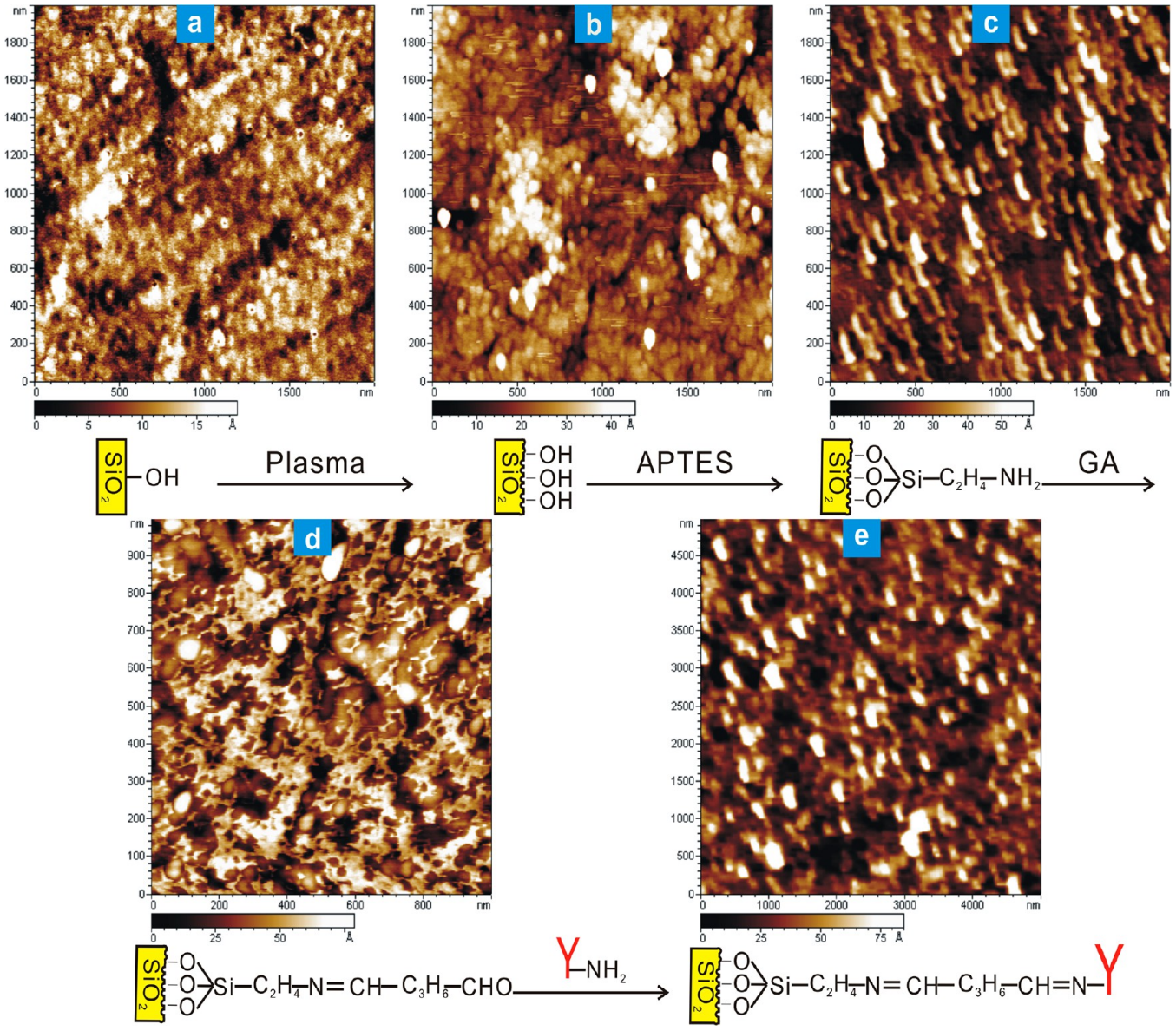

Figure 4. AFM images of the antibody immobilization process and the corresponding schemes of the stepwise procedures. (a) Bare silica slice. (b) The same silica slice shown in part a but after H_2O/Ar plasma pretreatment. (c) The silica slice shown in part b after reaction with APTES. (d) The silica slice shown in part c after reaction with GA. (e) The silica slice shown in part d after CEA antibody immobilization.

sodium line (589.1 nm) may have been introduced into the plasma system by accident.

It is thought that the introduction of water vapor into the microwave-induced H_2O/Ar plasma generated hydroxyl groups, which were then grafted onto the silica surface to form Si−OH. Thus, the OH radical was the focus of the remaining studies. Based on Figure 3, the possible mechanisms for the formations[32,36] of OH radicals on the silica surface are as follows: (1) water molecules dissociating into OH radicals and hydrogen radicals after electron impacts;

$$e + H_2O \rightarrow OH(X) + H(1s) + e \quad (1)$$

(2) OH radical production via collisions between water vapor and oxygen atoms;

$$e + O_2 \rightarrow O(^3P) + O(^1D) \quad (2)$$

$$O(^1D) + H_2O \rightarrow OH + OH + h\nu \quad (3)$$

(3) the dissociative recombination of water ions can be a major source of OH, due to the lower energy required than above possible reaction pathways;[32]

$$Ar^* + H_2O \rightarrow Ar + H_2O^+ \quad (4)$$

$$H_2O + e \rightarrow H_2O^+ \quad (5)$$

$$H_2O^+ + e \rightarrow OH + H \quad (6)$$

(4) recombination of H/OH and OH radicals to form water/hydrogen peroxide via three-body interactions, which had a role in the introduction of hydroxyl groups onto the surface.[32,36]

$$OH + OH + M \rightarrow H_2O_2 + M \quad (7)$$

$$H + OH + M \rightarrow H_2O + M \quad (8)$$

During the surface modification of the SiO_2 layer, OH radicals connected to the dangling bonds over the surface. However, the OH group would be removed from the SiO_2

dx.doi.org/10.1021/ac400226n | *Anal. Chem.* 2013, 85, 4578−4585

surface because of the atoms produced by the plasma etching effect.[36] The introduction of functional OH groups onto the silica surface was closely related to the concentration of OH radicals and atoms produced in the plasma. The concentration of the water molecules in the mixed gas was also of significant importance, and it was optimized to 2% (V/V) in our experiment (data not shown).

Another function of plasma was the etching effect, which can enhance antibody immobilization. The energetic electrons as well as hydrogen, oxygen, and Ar atoms, radicals, and ions in the plasma were accelerated toward the substrate, which produced defects and dangling bonds on the surface. The AFM images in Figures 4(a) and 4(b) show that a wavy morphology appeared, while the average roughness increased from 0.48 to 0.94 nm after the clean silica slice was treated using the microwave-induced H_2O/Ar plasma. This etching cleaned the substrate surface and left active sites for binding.[31] Those active sites can capture OH radicals formed with microwave induced H_2O/Ar plasma through eqs 7 and 8. The surface bond with OH serve as anchoring points and can conjugate to NHS ester of biotin or cross-linkers for antibody immobilization. Therefore, the quantity of the bonding OH on the silica surface and the antibodies immobilized increased with microwave induced H_2O/Ar plasma pretreatment compared to without it.

In summary, the microwave-induced H_2O/Ar plasma introduced large amounts of OH groups onto the SiO_2 surface, while the etching effect provided an activated surface for bonding so the surface provided better adhesion with other compounds, especially APTES. Thus, the immobilization of antibodies was enhanced after the plasma pretreatment.

Antibody Immobilization Enhancement with Plasma Pretreatment. AFM was used to monitor the surface morphology of the different surfaces in different antibody immobilization procedures. The two-dimensional AFM images of the five steps during the surface immobilization of the CEA antibody are shown in Figure 4. Figure 4(a) shows a bare silica slice, which has a flat profile with an average roughness of 0.48 nm and a maximum height of 20 Å. The morphology changed after the microwave-induced H_2O/Ar plasma treatment where the roughness and maximum height increased to 0.94 nm and 45 Å, respectively (Figure 4(b)). Unlike the flat profile of the silica slice, a wavy morphology was observed on the surface after plasma treatment because defects and hydroxyl groups were formed on the surface by the etching effect and the functionalization of plasma. In the next step, the images of the APTES-modified surface are shown in Figure 4(c). The effect of plasma treatment induced the organization of the APTES molecules and produced a uniformly distributed self-assembled monolayer, which was covalently bonded to the silica surface. As a result, the maximum height increased to 60 Å. Figure 4(d) shows the GA-functionalized surface. Incubation of the APTES-modified surface with GA produced surface topography changes and the appearance of bright snowflakes on top of the surface, with a maximum height of 75 Å. CEA antibody binding to the GA-functionalized surface was characterized by the formation of large features in the AFM image in Figure 4(e). The assembled modification of the antibodies was uniform, as shown by the complete coverage of the silica surface. The AFM image does not show single binding events between the amino groups of the antibody and aldehyde groups of GA at a molecular level, but they do support an interpretation that the features in Figure 4(e) were due to the antibody binding with its target. The variations in maximum height (increased from 75 to 85 Å) were consistent with the self-assembly of antibodies. Importantly, the results provide powerful evidence that validates enhanced antibody immobilization using this microwave-induced H_2O/Ar plasma pretreatment.

Analytical Performance of CEA Assays. The effectiveness of microwave-induced H_2O/Ar plasma during the production of the CEA immunosensor was characterized by assaying its analytical performance. Calibration curves (Figure 5) were constructed for a range of concentrations using CEA

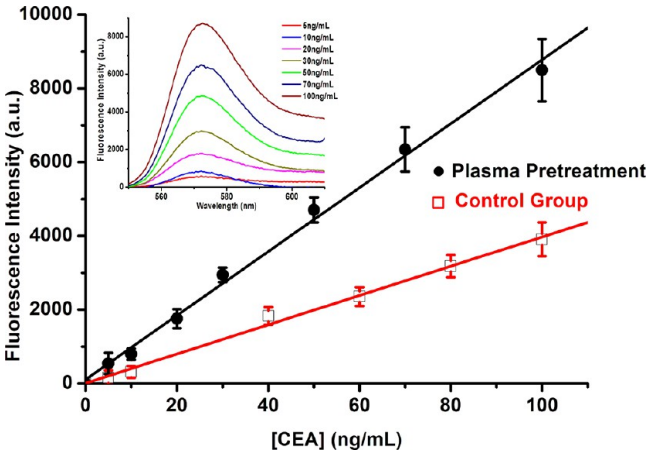

Figure 5. Linear and sensitive dose responses of CEA for plasma pretreatment group and control group with error bars (standard deviation from the mean, n = 6). Inset: Fluorescence spectra of the immunosensors with plasma pretreatment in the presence of different CEA concentrations (from bottom to top: 5, 10, 20, 30, 50, 70, 100 ng/mL). Excitation was set at 532 nm, and the emission intensity was monitored at 573.57 nm. All measurements were done in PBS buffer (0.01 M, pH 7.4).

antigen from human fluid in the buffer as well as a negative control, the zero calibration point for the plasma pretreatment group, and a control group where the capillary tubes were not pretreated with plasma. The best fit regression lines for the two groups were S = 87.669 × CEA + 110.85 (r = 0.9978) for the immunosensor with plasma pretreatment, and S = 39.659 × CEA + 6.9668 (r = 0.9975) for the control group, where S was the Cy3 fluorescent intensity signal, as described above. The sensitivity was defined as the slope of the line with the best fit, and it was at least two times higher with the plasma pretreatment compared that without. Importantly, the improved sensitivity during CEA immunosensor detection after plasma pretreatment demonstrated the efficiency of the plasma pretreatment process during antibody immobilization and its potential application for detecting trace amounts of biomarkers in samples.

The LOD was determined as $3\delta_b$/slope, which was 0.09 ng/mL for the plasma pretreatment and 0.2 ng/mL for the control group, compared with 1.2 ng/mL for an enzyme-linked immunosorbent assay (ELISA).[37] CEA is a glycosolated protein with a molecular weight of 180 kD so the LOD corresponded to 0.5 pmol/L. The LOD was below the commonly accepted disease diagnostic decision threshold for CEA in serum (2.5 ng/mL or 5 ng/mL for smokers).[37] The limit of quantification (LOQ), according to the definition of $10\delta_b$/slope, was 0.3 ng/mL for the immunosensor with plasma pretreatment and 0.67 ng/mL for control group. Importantly, this order of magnitude

dx.doi.org/10.1021/ac400226n | Anal. Chem. 2013, 85, 4578−4585

improvement in the LOD and LOQ using CEA immunosensor detection with plasma pretreatment demonstrated the stability of the plasma pretreatment approach to antibody immobilization and a laser-induced fluorescence immunosensor.

The immunosensor had a linear response at 0.3−100 ng/mL, which was an improvement of 10 times compared with a commercial ELISA with a linear range of 0.3−10 ng/mL. In this study, the linear range of the assay overlapped with the physiologically relevant range of analytes in biological samples. The wider linear range also indicated that the quantity of immobilized antibody was increased by the plasma pretreatment.

The reproducibility of the immunosensor was evaluated using intra-assay and interassay approaches. The intra-assay coefficient of variations (CVs) from three immunosensors for six replicate determinations were 3.5%, 4.1%, and 6.1% at 10, 50, and 70 ng/mL CEA, respectively. The interassay CVs measured using three immunosensors for six replicate determinations were 4.9%, 6.5%, and 7.2% at 10, 50, and 70 ng/mL CEA, respectively. These results indicated acceptable reproducibility and repeatability of the proposed immunosensor. To evaluate the precision between assays, two saliva samples (mean values were 28.16 and 38.2 ng/mL) were examined for six times. The CVs were 2.8 and 3.7%, whereas the variances with the ELISA approached 40%, depending on the analyte concentration.[37]

To investigate interference effect or crossing recognition level, some nonspecific proteins, amino acids, and drugs were used for testing this immunosensor, respectively. The analytical responses to each interference substance were evaluated. Figure 6 summarizes the interference at the presence of 2000 ng/mL

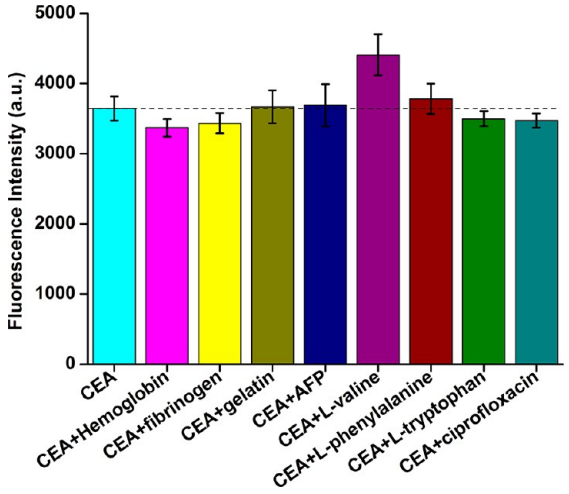

Figure 6. Interference effects of 2000 ng/mL various substances in a 40 ng/mL CEA solution with error bars (standard deviation from the mean, n = 5).

level of AFP, human fibrinogen, hemoglobin, gelatin, L-tryptophan, L-phenylalanine, L-valine, and ciprofloxacin added to the solutions containing 40 ng/mL CEA. The maximum signal increasing and suppression were observed in the presence of L-valine and hemoglobin, respectively. The former exhibited the most severe increasing and contributed to a 21% increase in the signal amplitude. The latter influenced about 8% of the original signal. The effects with AFP, gelatin, human fibrinogen, ciprofloxacin, L-tryptophan, and L-phenylalanine were negligible. This immunosensor showed strong anti-interference capability because of the specific binding between antibodies and antigens.

To evaluate the recovery (accuracy) with the method, blank samples were spiked at three concentrations and analyzed three times. The relative mean recovery ranged from 99.7% to 107.1% (see Table S-1 in the Supporting Information).

Analytical Performance of CEA Assays Using Clinical Samples. In the initial stages of these clinical proof-of-principle studies, the signal generated by saliva was compared to the CEA antigen from human fluid in a buffer. We analyzed CEA antigen (30 ng/mL), saliva, saliva spiked with CEA antigen (plus 30 ng/mL), and saliva depleted of protein by treatment in a water bath for 1 h followed by centrifugation at 15500 r/min for 20 min. The results are shown in Figure 7. The

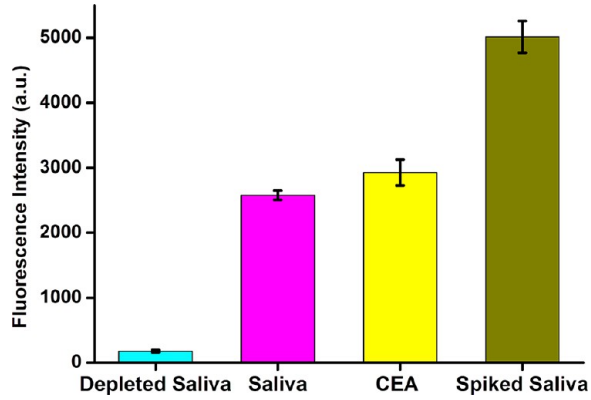

Figure 7. Validation of an authentic CEA signal in saliva with error bars (standard deviation from the mean, n = 3). CEA (30 ng/mL), saliva, saliva sample spiked with CEA, and depleted saliva indicates that a signal in saliva is authentic to CEA.

presence of a signal in saliva, signal increase after spiking with antigen, and signal decrease after depleted of protein offer powerful evidence for the validity of the assay and the authenticity of a CEA-specific signal in saliva.

The CEA immunosensor was used for CEA detection in saliva. Whole saliva was collected from apparently healthy nonsmoking subjects and the specimens were analyzed using the CEA immunosensor and compared with electrochemiluminescence immunoassay (ECL) measured by independent ADICON clinical laboratory Inc. (Chengdu, China). The methods correlate strongly with an R^2-value of 0.95 for human saliva CEA measurement in the range of 0−90 ng/mL (see Figure 8). The CEA concentrations of analytes present in saliva were consistent with previous reports[37−39] and the results were reasonable compared with the disease diagnostic decision thresholds of CEA in saliva (35 ng/mL) for normal individuals according to Chen's group,[40] because CEA is known to be an epithelial protein. The RSD values were <5% for all saliva samples and illustrated the potential to affect positive patient outcomes through saliva-based measurements.

CONCLUSION

This study demonstrated the possibility of antibody immobilization using microwave-induced H_2O/Ar plasma pretreatment. Microwave-induced H_2O/Ar plasma introduced large amounts of hydroxyl groups onto the SiO_2 surface and etched the surface to provide activated sites for bonding, so the surface provided better adhesion with antibodies. Furthermore, performance improvements were found obviously with

dx.doi.org/10.1021/ac400226n | Anal. Chem. 2013, 85, 4578−4585

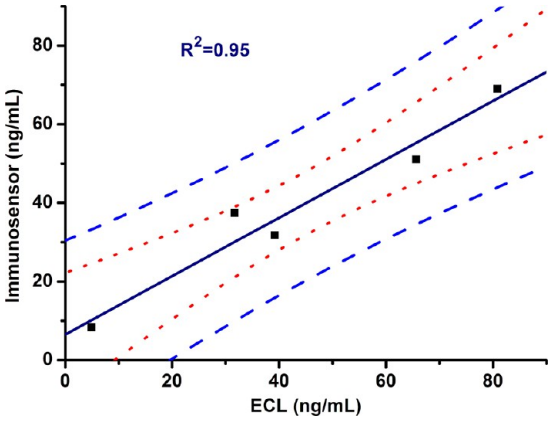

Figure 8. Correlation between ECL and our assays (n = 6). In addition to best-fit line (solid), the 95% confidence interval (dot) and 95% prediction interval (dash) are presented.

plasma-enhanced CEA immunosensor, including sensitivity, LOD, and linear dynamic range. This novel technique expands the applications of plasma and provides a new solution for antibody immobilization.

The construction and validation of a CEA immunosensor based on surface pretreatment using microwave-induced H_2O/Ar plasma is an important contribution toward the development of a harmonized tumor marker analysis system. The immunosensor was constructed using a sandwich immunoassay format after the surface was activated by plasma to enhance the immobilization of a capture antibody. To the best of our knowledge, this is the first study where microwave induced H_2O/Ar plasma was used for antibody immobilization, and we also provided quantitative CEA information using clinical salivary samples. The detection sensitivity was increased by at least two times, and the LOD was improved to 0.5 pmol/L after plasma pretreatment. Importantly, the linear dynamic range increased 10 times, which makes this approach more suitable for clinical practice than ELISA. The plasma-enhanced CEA immunosensor has validated clinical advantages including high sensitivity, a wide linear range that is suitable for clinical testing, a low LOD that is essential for clinical analysis, good reproducibility, and acceptable accuracy. Thus, interesting applications of plasma such as surface-specific functionalization and sensitive cancer diagnostic tool construction are close to real utilization based on this study.

■ ASSOCIATED CONTENT

Supporting Information

Additional information as noted in text. This material is available free of charge via the Internet at http://pubs.acs.org.

■ AUTHOR INFORMATION

Corresponding Author

*E-mail: yduan@scu.edu.cn.

Notes

The authors declare no competing financial interest.

■ ACKNOWLEDGMENTS

The authors acknowledge funding provided by the National Natural Science Foundation of China (No. 21275105), the National Major Scientific Instruments and Equipments Development Special Funds (No. 2011YQ030113), and the National Recruitment Program of Global Experts (NRPGE). We thank Miss Xin Yuan for her assistance in the preparation of this article.

■ REFERENCES

(1) Pei, X.; Chen, B.; Li, L.; Gao, F.; Jiang, Z. *Analyst* **2010**, *135*, 177−181.
(2) Gong, H.; Cradduck, M.; Cheung, L.; Olive, D. M. *Anal. Biochem.* **2012**, *426*, 27−29.
(3) Niotis, A.; Mastichiadis, C.; Petrou, P.; Christofidis, I.; Kakabakos, S.; Siafaka-Kapadai, A.; Misiakos, K. *Anal. Bioanal. Chem.* **2010**, *396*, 1187−1196.
(4) Niotis, A.; Mastichiadis, C.; Petrou, P.; Christofidis, I.; Siafaka-Kapadai, A.; Misiakos, K.; Kakabakos, S. *Anal. Bioanal. Chem.* **2009**, *393*, 1081−1086.
(5) Patel, R.; Vetter, E. A.; Harmsen, W. S.; Schleck, C. D.; Fadel, H. J.; Cockerill, F. R., 3rd *J. Clin. Microbiol.* **2011**, *49*, 4047−4051.
(6) Bhatia, S. K.; Shriver-Lake, L. C.; Prior, K. J.; Georger, J. H.; Calvert, J. M.; Bredehorst, R.; Ligler, F. S. *Anal. Biochem.* **1989**, *178*, 408−413.
(7) Zhou, L.; Ding, F.; Chen, H.; Ding, W.; Zhang, W.; Chou, S. Y. *Anal. Chem.* **2012**, *84*, 4489−4495.
(8) Li, H.; Cao, Z.; Zhang, Y.; Lau, C.; Lu, J. *Analyst* **2011**, *136*, 1399−1405.
(9) Bergström, G.; Mandenius, C.-F. *Sens. Actuators, B* **2011**, *158*, 265−270.
(10) Zhao, X. B.; Pan, F.; Cowsill, B.; Lu, J. R. *Langmuir* **2011**, *27*, 7654−7662.
(11) Feng, L. *Glass* **1986**, 39−42.
(12) Wang, C.; Srivastava, N.; Scherrer, S.; Jang, P.-R.; Dibble, T. S.; Duan, Y. *Plasma Sources Sci. Technol.* **2009**, *18*, 025030.
(13) Duan, Y.; Huang, C.; Yu, Q. *IEEE Trans. Plasma Sci.* **2005**, *33*, 328−329.
(14) Duan, Y. X.; Wang, C. J.; Scherrer, S. T.; Winstead, C. B. *Anal. Chem.* **2005**, *77*, 4883−4889.
(15) Tang, J.; Zhao, W.; Duan, Y. *Plasma Sources Sci. Technol.* **2011**, *20*, 045009.
(16) Jin, Z.; Duan, Y. *Rev. Sci. Instrum.* **2003**, *74*, 5156−5160.
(17) Liu, Y.; Cao, W.; Ding, X.; Yuan, X.; Duan, Y. *Spectrochim. Acta, Part B* **2012**, *76*, 152−158.
(18) Yuan, X.; Tang, J.; Duan, Y. *Appl. Spectrosc. Rev.* **2011**, *46*, 581−605.
(19) Mirabedini, S. M.; Arabi, H.; Salem, A.; Asiaban, S. *Prog. Org. Coat.* **2007**, *60*, 105−111.
(20) Ricard, A.; Gaboriau, F.; Canal, C. *Surf. Coat. Technol.* **2008**, *202*, 5220−5224.
(21) Moriceau, H.; Rieutord, F.; Morales, C.; Charvet, A. M. *Microsyst. Technol.* **2006**, *12*, 378−382.
(22) Tuleta, M. *Acta Phys. Pol., A* **2011**, *120*, 91−93.
(23) Denisenko, A.; Romanyuk, A.; Pietzka, C.; Scharpf, J.; Kohn, E. *J. Appl. Phys.* **2010**, *108*, 074901.
(24) Lim, H. R.; Baek, H. S.; Lee, M. H.; Woo, Y. I.; Han, D.-W.; Han, M. H.; Baik, H. K.; Choi, W. S.; Park, K. D.; Chung, K.-H.; Park, J.-C. *Surf. Coat. Technol.* **2008**, *202*, 5768−5772.
(25) Brueckner, S.; Hoffmeister, J.; Ihlemann, J.; Gerhard, C.; Wieneke, S.; Vioel, W. *J. Laser Micro/Nanoeng.* **2012**, *7*, 73−76.
(26) Baek, H. S.; Park, Y. H.; Ki, C. S.; Park, J.-C.; Rah, D. K. *Surf. Coat. Technol.* **2008**, *202*, 5794−5797.
(27) Gan, B. K.; Kondyurin, A.; Bilek, M. M. M. *Langmuir* **2007**, *23*, 2741−2746.
(28) Shao, Z. Y.; Ogino, A.; Nagatsu, M. *Jpn. J. Appl. Phys.* **2011**, *50*, 08JF03.
(29) Gauvreau, V.; Chevallier, P.; Vallieres, K.; Petitclerc, E.; Gaudreault, R. C.; Laroche, G. *Bioconjugate Chem* **2004**, *15*, 1146−1156.
(30) Chen, C.; Liang, B.; Ogino, A.; Wang, X.; Nagatsu, M. *J. Phys. Chem. C* **2009**, *113*, 7659−7665.
(31) Gao, J.; Chan-Park, M. B. *Surf. Coat. Technol.* **2005**, *194*, 244−250.
(32) Srivastava, N.; Wang, C. *J. Appl. Phys.* **2011**, *110*, 053304.

(33) Navazesh, M. *J. Am. Dent. Assoc.* **2003**, *134*, 613−618.
(34) Wang, C.; Mazzotti, F. J.; Koirala, S. P.; Winstead, C. B.; Miller, G. P. *Appl. Spectrosc.* **2004**, *58*, 734−740.
(35) Sun, M.; Wu, Y.; Li, J.; Wang, N. H.; Wu, J.; Shang, K. F.; Zhang, J. L. *Plasma Chem. Plasma Process.* **2005**, *25*, 31−40.
(36) Shao, Z.; Ogino, A.; Nagatsu, M. *Appl. Phys. Exp.* **2012**, *5*, 046201.
(37) Jokerst, J. V.; Raamanathan, A.; Christodoulides, N.; Floriano, P. N.; Pollard, A. A.; Simmons, G. W.; Wong, J.; Gage, C.; Furmaga, W. B.; Redding, S. W.; McDevitt, J. T. *Biosens. Bioelectron.* **2009**, *24*, 3622−3629.
(38) Vahedi, M.; Abdollahzadeh, S.; Vaziri, P. B.; Mortazavi, H. *Med. Oral Patol. Oral Cir. Bucal* **2011**, *16*, E29−E32.
(39) Brooks, M. N.; Wang, J. G.; Li, Y.; Zhang, R.; Elashoff, D.; Wong, D. T. *Mol. Med. Rep.* **2008**, *1*, 375−378.
(40) Chen, G.; Sun, C.; Yan, J.; Chen, J.; Zhang, X. *J. Pract. Oncol.* **1993**, *8*, 94−95.